Journal of Hazardous Materials 169 (2009) 271–278

Contents lists available at ScienceDirect

Journal of Hazardous Materials

journal homepage: www.elsevier.com/locate/jhazmat

Valorisation of wastewater from two-phase olive oil extraction in fired clay brick production

José A. de la Casa [a], Miguel Lorite [b], Juan Jiménez [b], Eulogio Castro [c,*]

[a] Cerámica Malpesa, S.A. Autovía A-4, km 303, 23710 Bailén (Jaén), Spain
[b] Department of Geology, University of Jaén, 23071 Jaén, Spain
[c] Department of Chemical, Environmental and Materials Engineering, University of Jaén, 23071 Jaén, Spain

ARTICLE INFO

Article history:
Received 5 February 2009
Received in revised form 18 March 2009
Accepted 19 March 2009
Available online 27 March 2009

Keywords:
Ceramic building materials
Olive mill wastewater
Two-phase olive oil extraction
Physical properties

ABSTRACT

Wastewater issued from oil-washing stage (OWW) in the two-phase olive oil extraction method was used to replace fresh water in clay brick manufacture. The extrusion trials were performed with one of the ceramic bodies currently being used in a local brick factory for red facing bricks (RB) production. Fresh water or OWW was added to a final consistency of 2.4 kg/cm^2, the same value as used at industrial scale for this kind of clay mixture. Comparative results of technological properties of facing bricks are presented. Results show that the products obtained with olive oil wastewater are comparable to traditional ones in terms of extrusion performance and technological properties of end products. Even dry-bending strength of the body formed by wastewater improves by 33% compared to fresh water body. In addition, heating requirements can be reduced in the range 2.4–7.3% depending on the final product. This application can alleviate environmental impacts from the olive oil extraction industry and, at the same time, result in economic savings for the brick manufacturing industry.

1. Introduction

Olive oil production is one of the most important agricultural industries in the Mediterranean basin countries, Spain being one of the first olive oil producers in the world. Contrary to other top olive oil producers, the olive oil extraction method used in Spain is the so-called "two-phase" method, in which a solid fraction, wet pomace or "alperujo", and a liquid one (the olive oil itself) are obtained. The extraction method in the other olive oil producing countries is the three-phase one, in which a solid fraction (wet pomace), a liquid residue, and the olive oil are obtained. The main advantage of the two-phase system is the reduction of olive mill wastewater amount, as most of the process water and olive fruit vegetation water enters the solid waste. Nevertheless, olive oil production still generates some wastewater coming out basically from washing of both the fruits (before entering the extraction process) and the olive oil (in the late centrifugation wash). This wastewater has a high polluting charge and is typically sent to evaporation ponds. This common elimination method requires relatively large evaporation surfaces, with associated investment costs including impermeability treatments, and may cause environmental problems like bad odour, infiltration and insect proliferation [1]. Available studies on olive mill wastes [2] have focused basically on alperujo [3,4] or its valorisation [5–7] concerning the solid waste fraction, and three-phase wastewater treatment [8–11] concerning the liquid waste fraction, but there is little information on disposal alternatives for two-phase olive mill wastewater, in spite of being produced at large amounts every year. It has been estimated that every ton of processed olive fruits by such an extraction configuration generates around 200 L wastewater [1]. Taken into account that Spain's olive production was about 5,000,000 tons in 2006 [12], it can be concluded that two-phase olive wastewater production is high enough to deserve a study on disposal alternatives. Recently a review on chemical treatment technologies of liquid and solid wastes from two-phase olive oil mills was published by Borja et al. [13].

The use of three-phase olive mill wastewater in the manufacture of fired clay bricks has been previously reported [14,15].

This work deals with the use of two-phase olive mill wastewater for building materials production. The objective of the work is to assess whether (1) oil-washing wastewater can be used to replace fresh water and (2) the physical and mechanical properties of facing bricks obtained by using this wastewater are comparable to those of fresh-water facing bricks. The experimental work has been performed in collaboration with a reference brick making industry located at Bailén (Jaén, Spain). The ceramic industry in the Bailén area is the most important centre of heavy clay products in southern Spain. Most of the factories are given over to the production of common bricks, using almost exclusively the tertiary

* Corresponding author. Tel.: +34 953212163; fax: +34 953212141.
E-mail address: ecastro@ujaen.es (E. Castro).

0304-3894/$ – see front matter © 2009 Elsevier B.V. All rights reserved.
doi:10.1016/j.jhazmat.2009.03.095

Table 1
XRD mineralogical characterization of the used clay.

	Phyllosilicates	Quartz	Calcite	Dolomite	Feldspars
Whole composition	59	30	9	Traces	Traces
Clay minerals		Illite 60	Kaolinite 35	Pyrophyllite 5	Smectite –

Table 2
Chemical composition (oxide content, %) of the used clay.

Oxide content (%)										
SiO_2	Al_2O_3	Fe_2O_3	MnO	MgO	CaO	Na_2O	K_2O	TiO_2	P_2O_5	LOI
53.27	15.97	6.39	0.06	1.92	5.88	0.4	3.82	0.77	0.14	9.69

LOI: loss on ignition.

materials from the Guadalquivir basin. The potential uses of these raw materials and mixtures of them with commercial products have been established in previous works [16,17]. The building materials industry has been used as recipient for residues from many other production sectors, e.g. petroleum residues [18], ashes from activated sludge urban wastewater plants [19] and granite residues [20].

2. Materials and methods

2.1. Clay

The used clay was provided by Cerámica Malpesa, S.A. (Bailén, Spain), a local ceramic industry. The chemical composition and the mineralogical characterization of the clay are summarized in Tables 1 and 2, respectively.

2.2. Olive mill wastewater characterization

Oil-washing wastewater (OWW) was collected from the oil-washing vertical centrifuge in a local industry operating two-phase olive oil extraction method. The composition of olive mill wastewater depends on several factors, e.g. operation conditions, olive variety, and olive maturation grade, among others [13]. The main physico-chemical features of the used olive mill wastewater are presented in Table 3.

The calcite content of the clay was 9%, so taken into account that the OWW acidity was 680 mg $CaCO_3$ dm^{-3}, it can be concluded that there is enough calcite to neutralize the acidity of the water used for the extruding body.

Concerning the dry residue of the oil-washing wastewater (2.51%), the higher heating value (HHV) can be evaluated from the elemental composition by using the following equation proposed for several types of biomass [21]:

$$\mathrm{HHV(MJ/kg)} = -1.3675 + 0.3137 \cdot \mathrm{C} + 0.7009 \cdot \mathrm{H} + 0.0318 \cdot \mathrm{O}^{*}$$

where C and H stand for the weight percentage of carbon and hydrogen in the biomass on dry matter basis, and $O^{*} = 100 - C - H - \text{ash content}$. This equation can be used to determine whether or not the HHV of the wastewater can contribute significantly to the heat requirements during the fabrication process.

2.3. Extrusion trials, drying and firing bricks

The extrusion trials were performed with one of the ceramic bodies currently being used in Cerámica Malpesa, S.A. for red facing bricks (RB). The mixture of clays was taken from the milling device of the industrial plant and was passed through shaking screens provided with 1.0 mm × 1.2 mm rectangular holes. The moisture content of the milled clay was typically 6–10%. The ceramic body for extrusion was prepared by mixing the clay mixture with fresh water (FW) or OWW in a lab mixer. The time elapsed from water addition to the beginning of the extrusion trial was around 2 h.

The amount of added water in the mixer depends on the clay plasticity and on the consistency at which the extrusion is performed. For soft extrusions, the clay consistency is usually in the range of 1.2–1.8 kg/cm^2 (as measured by a 6.35 mm in diameter penetrometer). For stiff extrusions, the consistency ranges from 3.0 to 4.5 kg/cm^2. The moisture content for stiff extrusion is 15–20%, and 21–26% for soft extrusions [22]. In the present work, fresh water or OWW was added to a final consistency of 2.4 kg/cm^2, the same value as used at industrial scale for this kind of clay mixture. Barium carbonate was also added for preventing scumming during the drying of test pieces. A rate of 1% (w/w) of a barium carbonante suspension having 70% solids (w/w) was used.

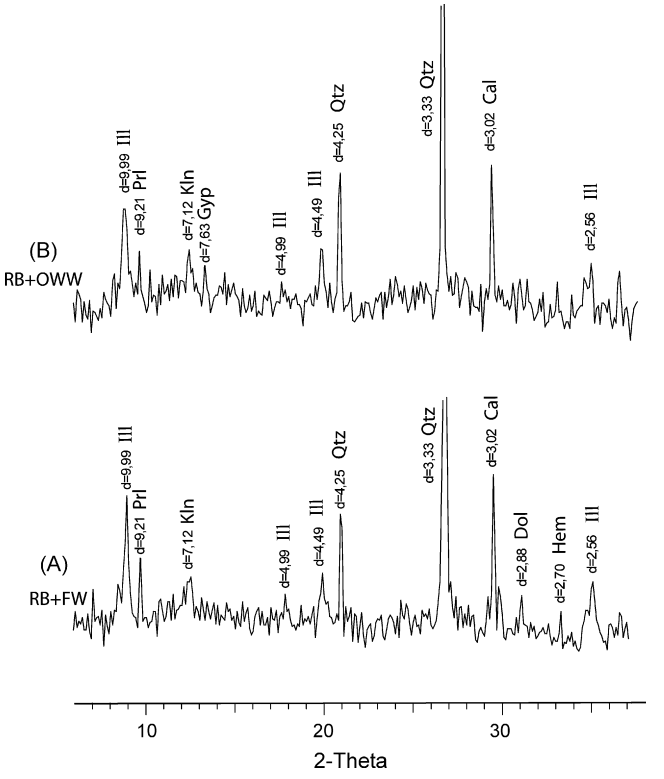

Fig. 1. X-ray diffraction patterns of the used clay raw mixtures. (A) RB + FW mixture; (B) RB + OWW mixture. Mineral symbols according to [34]. Ill: illite; Prl: pyrophyllite; Kln: Kaolinite; Qtz: quartz; Cal: calcite; Dol: dolomite; Gyp: gypsum; Hem: hematite.

Table 3
Physico-chemical characterization of the used olive oil wastewater and those of the dry residue.

OWW						Dry residue				
pH	Acidity to pH = 8.3 ($mg\ CaCO_3/dm^{-3}$)	Density ($kg\ dm^{-3}$)	Electrical conductivity ($mS\ cm^{-1}$)	Dry residue (%)	COD ($mg\ dm^{-3}$)	Organic matter (%)	Ashes (%)	C (%)	H (%)	N (%)
5.17	680	1.012	3.04	2.51	7840	92.03	7.97	47.53	5.77	0.73

The clay mixture was extruded using a lab vacuum extruder provided with manual cutter (Verdés 050-C, Barcelona, Spain). The ceramic rods were obtained under 91–92% vacuum and were approximately of 130 mm × 30 mm × 18 mm. Extruded test pieces were identified and weighted for moisture determination; finally the upper face of each test piece was indented at 100 mm spacing marks for ulterior drying and firing shrinkage determinations.

Extruded test pieces (RB + FW or RB + OWW) were dried at room temperature for about 12 h and then in an increasing temperature oven until reaching 110 °C in 8 h before constant weight for at least 24 h. Dried rods were fired in four trials: (a) electric lab furnace at 1000, 1025 and 1050 °C, and (b) gas-fired tunnel kiln, in a 24 h firing cycle at 1020 °C, according to the industrial firing cycle. The firing in electric furnace at 1025 °C is equivalent to tunnel kiln firing at 1020 °C, as verified by Bullers ring firing under both cycles. Enough test pieces were extruded, dried and fired to perform every test in six or ten test-piece samples and mean results are reported.

2.4. Analytical methods

The acidity of the OWW was determined according to UNE 77035:1983 standard. The electrical conductivity was electrometrically measured. Chemical oxygen demand (COD) and dry residue composition were established through potassium dichromate digestion and elemental analysis, respectively.

All the samples were subjected to mineralogical and chemical analyses in order to characterize their compositions. The mineralogical features were determined using X-ray diffraction (XRD, Siemens D-5000 with Ni-filtered Cu Kα radiation: 35 kV and 35 mA) and scanning electron microscopy (SEM, Jeol JSM-5800) with EDS microanalyser (Oxford Link). The XRD qualitative mineralogical analyses were carried out on bulk rock powder and <2 μm fractions. The clay minerals were detected on orientated aggregates (natural, ethylene glycol, dimethyl-sulfoxide solvated and heated at 550 °C for 2 h). Mineral identification was carried out by comparison with the Powder Diffraction File. The percentages of phyllosilicates were determined employing the mineral intensity factors published by Dinelli and Tateo [23]. Microtextural samples and clay microanalyses were studied by scanning electron microscopy. The following standards were used for calibration: albite, orthoclase, periclase, wollastonite and synthetic oxides (Al_2O_3, Fe_2O_3 and $MnTiO_3$). The chemical analyses of mayor oxides were performed using X-ray fluorescence spectrometry (Bruker S4 Pionner) on powder pellets.

XRD was also performed on the fired ceramic pieces to determine the high-temperature phases and SEM was also used to study the mineral phases formed and the microstructures.

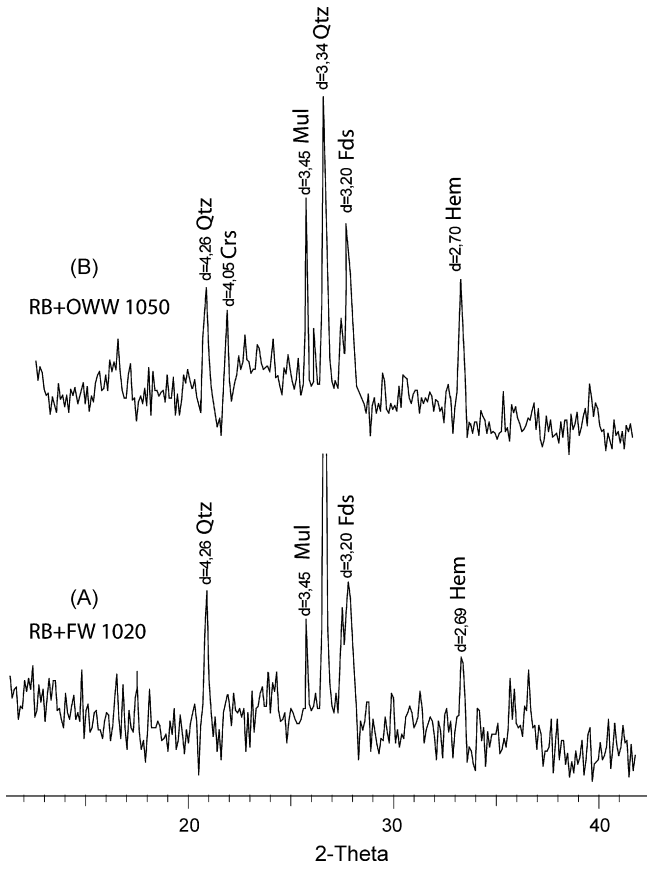

Fig. 2. X-ray diffraction patterns of fired bodies. (A) RB + FW mixture; (B) RB + OWW mixture. Mineral symbols according to [34]. Qtz: quartz; Crs: cristobalite; Mul: mullite; Fds: feldspars; Hem: hematite.

2.5. Additional tests

Several technological properties of the test pieces were determined according to established ceramic procedure as follows:

- The consistency of the rods was measured by using a ST 207 pocket penetrometer.
- The moisture content was determined by drying at 110 °C until constant weight.
- Linear drying and firing shrinkages were measured with an indent marker.
- The mass loss on firing was determined by weighing.
- Dried and fired rod strength was evaluated by three-point modulus of rupture with a universal MECMESIN 2500N Versatest machine.
- Water absorption was calculated according to Appendix C UNE-EN 771–1:2003 standard.
- Fired bulk density was determined following UNE-EN 772–13:2001 standard.
- Colour determinations (CIE Lab chromatic coordinates) were performed using a Minolta CR-300 colourimeter.

3. Results and discussion

3.1. Mineralogical and chemical composition of the raw materials

XRD data show that the raw clay materials mixture used to the elaboration of the ceramic pieces is rich in phyllosilicates with significant amounts of quartz and calcite (Table 1 and Fig. 1A). Dolomite and feldspars are also present in small quantities and traces of hematite can be observed. Illite is the main component of the clay mineral assemblage, although aluminium silicates such

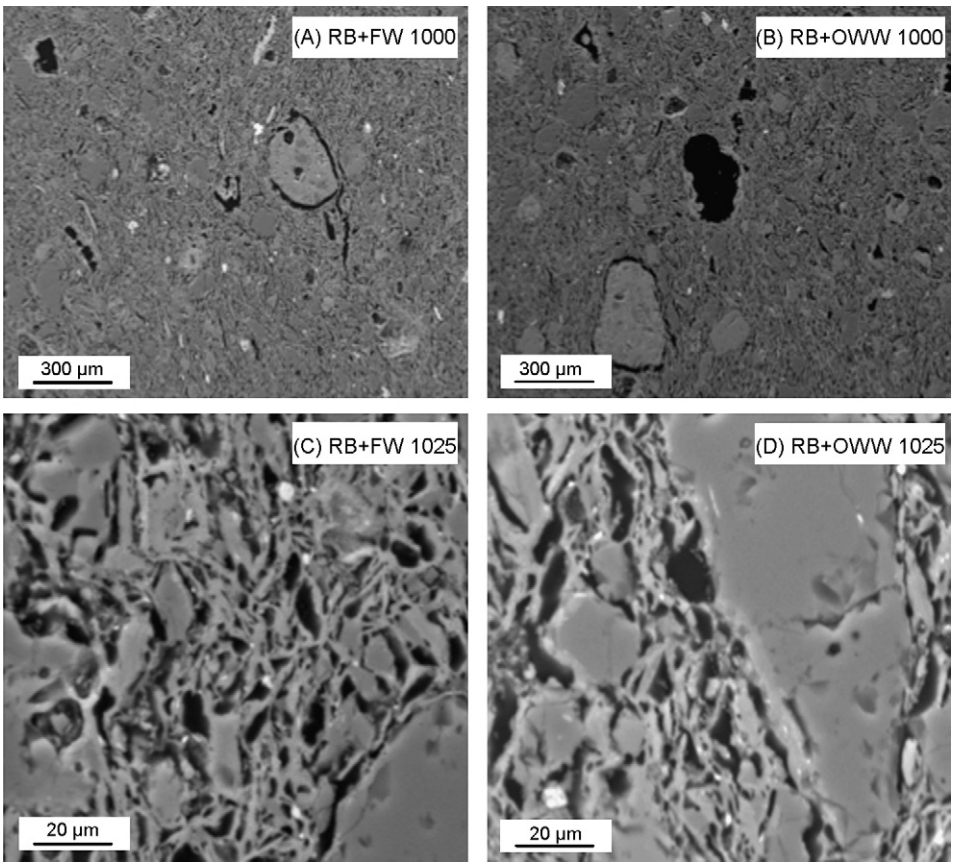

Fig. 3. Backscattered electron (BSE) images of scanning electron microscope in the atomic number contrast mode performed on polished samples from fired bodies.

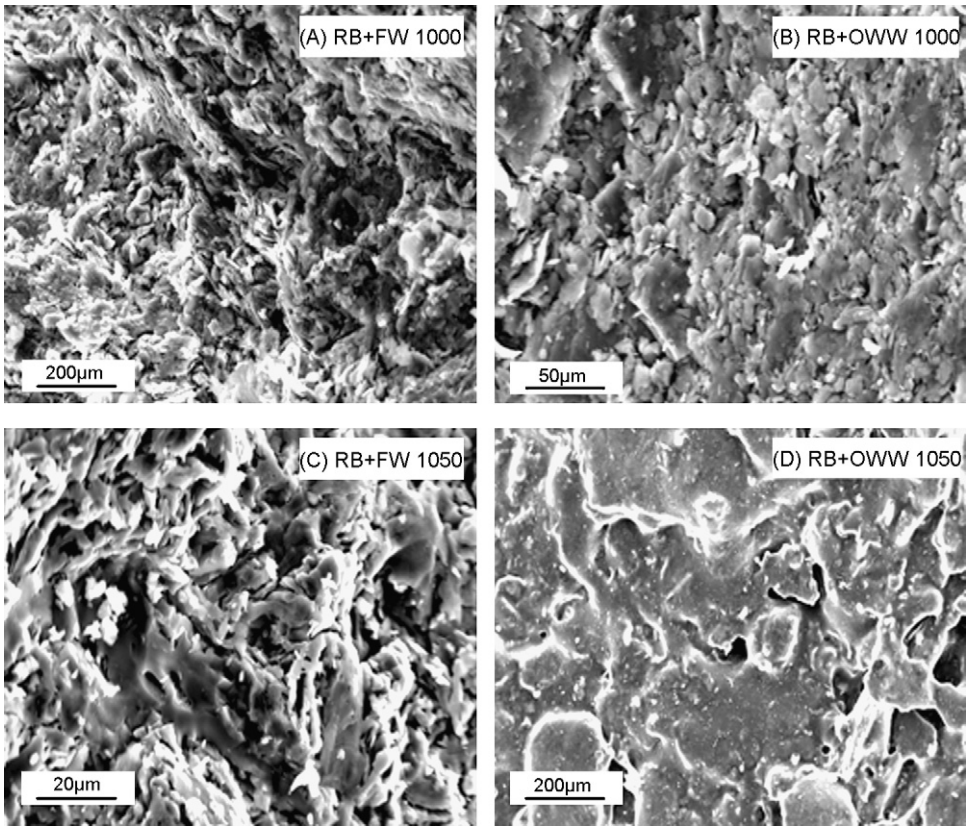

Fig. 4. Secondary electron (SE) images of scanning electron microscope from fired bodies.

as kaolinite and pyrophyllite have been identified in significant amounts.

The comparison of the mineralogical composition of the used mixture with the overall composition of common raw materials for ceramic products [24,25] reveals that this material contains the appropriated phyllosilicate, carbonate and quartz contents to be considered inside the range of mineralogical compositions potentially suitable for structural ceramic products.

According to its mineralogical composition, the raw material contains high amounts of silica (53.27%) and alumina (15.97%), mainly due to the illitic and kaolinitic and pyrophyllitic composition of this mixture (Table 2). The significant contents of CaO (5.88%) and Fe_2O_3 (6.39%) are related to the presence of calcite and hematite in the used mixture. The chemical composition of the mixture falls close to the field of illitic–chloritic clays used for making red stoneware and within the field of illitic–kaolinitic clays used for making white stoneware [26].

As regard the effect of the incorporation of olive mill wastewater to perform the ceramic pieces, XRD diagrams reveal a decrease of the dolomite amount present in the material and the presence of gypsum traces (Fig. 1B). This slight mineralogical difference can be related to the calcite dissolution process due to the introduction of the acid wastewater.

3.2. Mineralogical and textural characterization of the fired bodies

As concerns the mineralogical composition of the fired bodies determined by XRD (Fig. 2), the fired mineralogical assemblage consists mostly of mullite, hematite, cristobalite, feldspars and a vitreous phase. Traces of mullite are detected since 1000 °C. It has been observed that the higher the temperature, the greater the contents, size and crystallinity of mullite, which give the fired bodies greater strength. The hematite contents of the fired bodies are higher than those in the raw material samples, which suggests that part of the observed hematite is formed starting from 1000 °C at the expense of iron oxides produced by the breakdown of the phyllosilicates (mainly illite). The crystallisation of cristobalite has been observed at 1050 °C. It is well-known fact that the presence of this mineral is a drawback in the use of these raw materials, since it reduces the resistance of the fired bodies to thermal shock.

SEM images reveal some interesting aspects about the evolution of the microstructure and the mineralogy of the pieces with firing temperature. Clasts of silicate composition (especially quartz) of the previous raw materials always appear in the pieces at 1000 °C upwards (Fig. 3A). Several voids, probably reflecting the presence of carbonate clasts of the raw materials can also be observed (Fig. 3B). These voids develop rims of feldspars. Feldspars are also observed around quartz clasts (Fig. 3C) and forming the matrix of the fired pieces (Fig. 3D). The crystallisation of feldspars can be explained taking into account the destabilisation of carbonates present in the raw material according to the following reaction:

$$\underset{\text{Illite}}{KAl_2(Si_3Al)O_{10}(OH)_2} + \underset{\text{Calcite}}{CaCO_3} = +2\,SiO_2$$

$$\rightarrow \underset{\text{Sanidine}}{KAlSi_3O_8} + \underset{\text{Anhortite}}{CaAl_2Si_2O_8} + CO_2 + H_2O$$

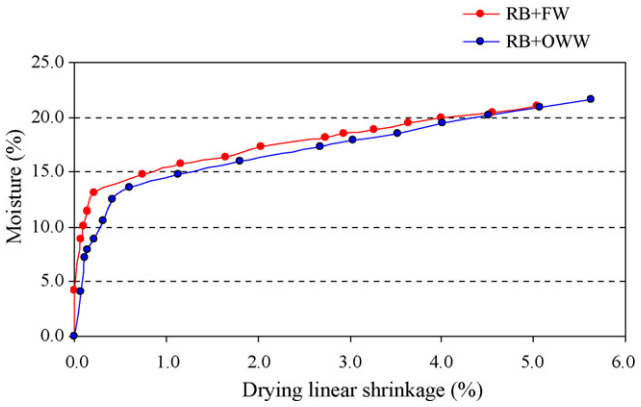

Fig. 5. Bigot's curve for RB + FW and RB + OWW bodies.

This reaction is the responsible of the high amount of anorthite of the fired pieces, which acts as sink for the Ca available in the raw material.

Fig. 4 shows that the earliest stage of vitrification is observed at 1000 °C. At this temperature, although the laminar aggregates of the clay minerals can still be recognised, the presence of some dispersed glassy filaments can be observed (Fig. 4A and B). At 1050 °C, the percentage and the size of the vitreous filaments increase, giving rise to areas with a texture characterized by the presence of elongated pores, due to the coalescence of clay minerals (Fig. 4C), although areas with a continuous vitreous matrix are also observed (Fig. 4D).

We have not found significant differences in the mineralogical composition and textural evolution in the samples prepared with olive mill wastewater.

3.3. Drying tests

The test piece behaviour in drying conditions, as evaluated by Bigot's curve, Nosova index and maximum limit of cracking, was evaluated on 200 mm × 80 mm × 9 mm fresh water and OWW extruded rods.

3.3.1. Bigot's curve

The Bigot's curves are normally used as routine control in traditional clay-based ceramic production for testing the sensitivity of clays and bodies to drying [27]. As shown in Fig. 5, the Bigot's curve represents the evolution of the linear shrinkage as a function of body moisture. For each depicted curve, the point with the highest moisture content stands for the beginning of the drying process. The required moisture for moulding includes two types [28]: (a) the so-called colloidal water or shrinkage water, situated among the particles and facilitating moulding, which is necessary to provide clay plasticity and is related to the specific surface of the body, being the main shrinkage factor, and (b) the porosity water or interstitial water, which is related to the attainable compaction.

Table 4
Maximum limit of cracking.

	Drying conditions			RB + FW	RB + OWW
	Temperature (°C)	Time (h)	Air speed ($m\,s^{-1}$)	Maximum limit of cracking (cm)	
Test piece 1	21	48	0	20	20
Test piece 2	21	24	1	20	20
Test piece 3	10–110	2	6	20	20
Test piece 4	75–120	3	6	20	20

Three phases can be observed during the drying process [29]. In the first one, water is evaporated at a constant rate. Both the superficial and inner temperatures of the ceramic piece and that of the drying air are different. At the beginning of the drying process the linear shrinkage is proportional to the evaporated water, and most of the shrinkage takes place. This shrinkage was approximately 5 and 4% for RB + OWW and RB + FW, respectively. The *Y*-axis interception of the linear part of the Bigot's curve determines the Critical Moisture Content (CMC), which is the theoretical moisture content beyond which no longer shrinkage is observed. The CMC values determined for RB + OWW and RB + FW were around 13 and 14%, respectively.

In the second drying phase, both the superficial and inner temperatures of the ceramic piece raise, approaching the drying air temperature. In this stage, drying shrinkage is not proportional to the evaporated water. Finally, there is no shrinkage during the third drying phase, and the remaining water is eliminated. At the end of this phase, the piece temperature equals the air temperature.

RB + FW body shows a shrinkage water/porosity water ratio lower than those of RB + OWW body. This determines a higher drying sensibility for RB + OWW that can be evaluated through Nosova index and maximum limit of cracking determinations.

3.3.2. Nosova index and maximum limit of cracking

The Nosova index uses the shrinkage water/porosity water ratio to determine the body sensibility to drying. Nosova index values in the range 0.5–1 indicate that the body shows little drying sensibility; values in the range 1.0–1.5 represent average sensibility, and Nosova index greater than 2 are typical of very drying sensible bodies which crack easily while drying [30]. The Nosova index for the RB + FW and RB + OWW bodies were 0.70 ± 0.02 and 0.79 ± 0.10, respectively, which allows both bodies to be classified as low drying sensible bodies.

Concerning maximum limit of cracking, the maximum separation between two adjacent cracks, Table 4 shows that no fissures or cracks were detected during the drying process of the test pieces. Consequently, no problems are expected during the industrial drying of these bodies; this result has already been verified with RB + FW body.

3.4. Dilatometric curve

The dilatometric curves for RB + FW and RB + OWW bodies at 1025 °C are depicted in Fig. 6. In general, a similar behaviour is observed. A steady and soft expansion is detected until the quartz inversion $\alpha \rightarrow \beta$. Beyond this point (573 °C) the expansion rates increased reaching the maximum at 840 °C (1.21%) and 830 °C (1.16%) for RB + FW and RB + OWW bodies, respectively. At temperatures higher than 900 °C the vitrification was more important due to the illite content of the body. The shrinkage associated to vitrification was stopped because of the CO_2 release from the decomposition of the carbonate content of the bodies. This shrinkage is more intense for the RB + FW body. The final result is 1.49% shrinkage for RB + FW body, compared to 0.75% for RB + OWW body.

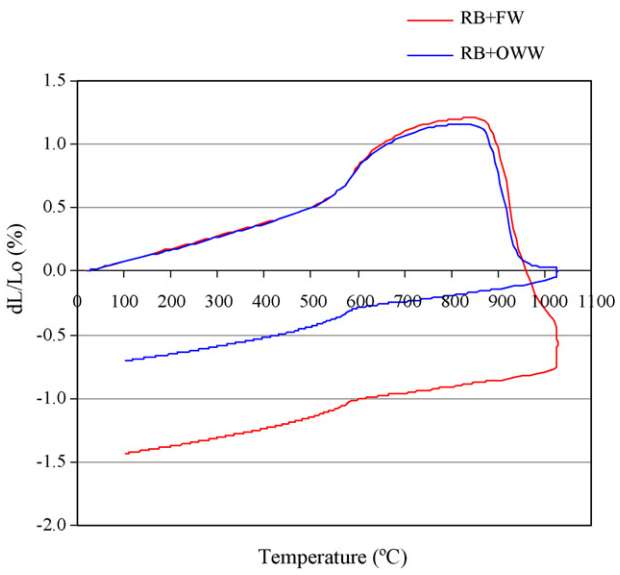

Fig. 6. Dilatometric curve for RB + FW and RB + OWW bodies at 1025 °C.

3.5. Technological properties of unfired bodies

The main results concerning technological properties of the unfired bodies are presented in Table 5 and briefly discussed bellow.

3.5.1. Consistency and moisture content

The working consistency was 2.4 kg cm^{-2}; it was obtained by a moisture content of 21.3% for RB + FW body and 21.9% for RB + OWW body. Taking into account that RB clay moisture was 6.8%, the weight percentage of added OWW was 15.1%.

3.5.2. Drying linear shrinkage

Similar values were obtained for both bodies.

3.5.3. Dry-bending strength

Dry-bending strength resulted 33% greater for RB + OWW body compared to that for RB + FW body. The effect of OWW on the dry-bending strength is similar to that caused by some additives that enhance plasticity. An increase from 6 to 11 N mm^{-2} was reported by using 0.5% by weight of such additives [31]. Nevertheless, the use of additives represents an additional cost [32] that can be eliminated by using OWW with the same effect. On the other hand, the values of dry-bending strength are high enough for the bricks to be manipulated for the usual furnace carrying systems, for which a minimum strength of 4.0 N mm^{-2} is required.

Table 5
Technological properties of unfired bodies.

Clay body	Firing temperature (°C)	Penetrometer consistency (kg cm^{-2})	Moisture content (%)	Drying linear shrinkage (%)	Dry-bending strength (N mm^{-2})
RB + FW	1000 (furnace)	2.4	21.0 ± 0.2	4.6 ± 0.1	6.0
	1025 (furnace)	± 0.1	21.0 ± 0.3	4.6 ± 0.1	± 0.3
	1050 (furnace)		21.1 ± 0.2	4.6 ± 0.1	
	1020 (tunnel kiln)		21.3 ± 0.2	4.5 ± 0.2	
[3,0]RB + OWW	1000 (furnace)	2.4	20.5 ± 0.2	4.0 ± 0.2	8.0
	1025 (furnace)	± 0.1	20.2 ± 0.6	3.9 ± 0.5	± 0.5
	1050 (furnace)		20.3 ± 0.5	4.0 ± 0.4	
	1020 (tunnel kiln)		21.9 ± 0.1	4.6 ± 0.1	

Table 6
Technological properties of fired test pieces.

Clay body	Firing temperature (°C)	Firing linear shrinkage (%)	Mass loss on firing (%)	Water absorption (%)	Fired bulk density ($kg\,m^{-3}$)	Fired-bending strength ($N\,mm^{-2}$)
RB + FW	1000 (furnace)	1.1 ± 0.1	7.89 ± 0.02	8	1970	16.6 ± 1.3
	1025 (furnace)	1.3 ± 0.1	7.89 ± 0.03	8	2000	19.5 ± 1.1
	1050 (furnace)	1.5 ± 0.1	7.92 ± 0.02	7	2010	19.9 ± 1.7
	1020 (tunnel kiln)	1.3 ± 0.1	7.92 ± 0.01	8	1970	18.7 ± 0.9
RB + OWW	1000 (furnace)	0.5 ± 0.1	9.05 ± 0.04	11	1870	17.6 ± 1.0
	1025 (furnace)	0.5 ± 0.1	9.07 ± 0.02	10	1880	18.1 ± 1.3
	1050 (furnace)	0.6 ± 0.1	9.10 ± 0.01	10	1900	18.0 ± 1.1
	1020 (tunnel kiln)	0.6 ± 0.1	9.08 ± 0.01	11	1870	16.8 ± 0.9

3.6. Technological properties of fired bodies

Table 6 summarizes the technological properties of RB + FW and RB + OWW fired bricks.

3.6.1. Firing linear shrinkage

Bodies formed by FW present a higher linear shrinkage than OWW bodies at any firing temperature. This result agrees with that found in the dilatometric assay. Moreover, the linear shrinkage dependence with firing temperature is more pronounced for FW body.

3.6.2. Mass loss on firing

Mass loss is due to firing reactions resulting in compound decomposition, organic matter combustion and so on. The higher organic matter of the OWW produces a higher mass loss at firing (15%) compared to FW bricks.

3.6.3. Water absorption

RB + OWW body presents lower firing linear shrinkages and greater mass losses than RB + FW body; accordingly, water absorption is greater in RB + OWW body at any firing temperature.

3.6.4. Fired bulk density and fired bending strength

These properties are slightly lower for RB + OWW bricks, due to a greater porosity of the bodies.

3.6.5. Black core

Additives, such as plastic clays, are sometimes used in brick manufacturing to enhance plasticity or to increase strength. The presence of organic matter in clays can cause a firing defect known as black core if the organic carbon is not completely burnt during firing. Factors favouring black core occurrence are a high organic matter and the vitrification of the brick, which can hinder combustion of the organic matter. No black core defect was observed for RB + FW nor RB + OWW bricks.

3.6.6. Brick colour

Colour is an important property for masonry units used without covering like facing bricks.

Table 7
Colour of fired test pieces.

Clay body	Firing temperature, °C	L^*	a^*	b^*
[3,0]RB + FW	1000 (furnace)	52.5 ± 0.2	23.1 ± 0.1	25.1 ± 0.2
	1025 (furnace)	51.7 ± 0.2	22.5 ± 0.1	23.7 ± 0.2
	1050 (furnace)	50.6 ± 0.3	21.6 ± 0.5	22.3 ± 0.5
	1020 (tunnel kiln)	51.9 ± 0.2	22.1 ± 0.1	23.1 ± 0.3
[3,0]RB + OWW	1000 (furnace)	54.2 ± 0.6	23.6 ± 0.1	26.2 ± 0.2
	1025 (furnace)	54.1 ± 0.3	22.8 ± 0.3	25.1 ± 0.3
	1050 (furnace)	53.5 ± 0.2	22.5 ± 0.2	24.7 ± 0.4
	1020 (tunnel kiln)	55.1 ± 0.1	22.4 ± 0.1	24.5 ± 0.3

Table 7 shows the chromatic ordinates obtained for both brick types. Values for RB + FW chromatic ordinates correspond to a deep red colour that gets darker as the firing temperature is increased; those of RB + OWW correspond to orange red and little differences are obtained as a function of firing temperature.

3.7. Higher heating value of OWW

Brick manufacturing includes usually some materials with variable organic matter content like clays, olive pomace or coke. For example, in the case of coke, with an average higher heating value of 32,000 kJ/kg, the addition of 1% by weight to the body represents 320 kJ/kg clay, equivalent to 10.7–32% of the heating requirements depending on the building product [33]. In the case of OWW, the higher heating value adds 73 kJ/kg clay, that is 2.4–7.3% of the heating requirements, which can be saved when OWW is used instead of fresh water for brick manufacturing.

4. Conclusions

Water used for olive oil washing in the late centrifuge step constitutes currently the main liquid residue obtained in most of olive oil extraction factories in Spain, operating the so-called two-phase extraction procedure. This highly pollutant residue is usually sent to evaporation ponds producing environmental concerns and an economical cost.

Disposal of wastewater obtained from olive oil extraction can be effectively achieved by using this liquid residue as mixing water for brick manufacturing, even in facing brick production. Mineral reactions during drying and firing experiments, as well as final technological properties are not affected by the use of the wastewater. Therefore, the acidity and the organic matter of the wastewater present no problems for such application. The main advantage for the olive oil extraction industry is the elimination of the aeration ponds for wastewater treatment, while building material industry benefits from reducing water and heating requirements, along with the production of equivalent or better materials.

References

[1] A. Roig, M.L. Cayuela, M.A. Sánchez-Monedero, An overview on olive mill wastes and their valorisation methods, Waste Manag. 26 (2006) 960–969.
[2] N. Azbar, A. Bayram, A. Filibeli, A. Muezzinoglu, F. Sengul, A. Ozer, A review of wastes management options in olive oil production, Crit. Rev. Environ. Sci. Technol. 34 (2004) 209–247.
[3] B. Rincón, E. Sánchez, F. Raposo, R. Borja, L. Travieso, M.A. Martín, A. Martín, Effect of the organic loading rate on the performance of anaerobic acidogenic fermentation of two-phase olive mill solid residue, Waste Manag. 28 (2008) 870–877.
[4] R. Borja, A. Martín, E. Sánchez, B. Rincón, F. Raposo, Kinetic modelling of the hydrolysis, acidogenic and methanogenic steps in the anaerobic digestion of two-phase olive pomace (TPOP), Process Biochem. 40 (2005) 1841–1847.
[5] J. Fernández-Bolaños, G. Rodríguez, R. Rodríguez, A. Heredia, R. Guillén, A. Jiménez, Production in large quantities of highly purified hydroxytyrosol from liquid-solid waste of two-phase olive oil processing or "Alperujo", J. Agric. Food Chem. 50 (2002) 6804–6811.

[6] J. Fernández-Bolaños, G. Rodríguez, E. Gómez, R. Guillen, A. Jimenez, A. Heredia, R. Rodríguez, Total recovery of the waste of two-phase olive oil processing: isolation of added-value compounds, J. Agric. Food Chem. 52 (2004) 5849–5855.
[7] G. Rodríguez, R. Rodríguez, A. Jiménez, R. Guillén, J. Fernández-Bolaños, Effect of steam treatment of alperujo on the composition, enzymatic saccharification, and in vitro digestibility of alperujo, J. Food Agric. Chem. 55 (2007) 136–142.
[8] S. Khoufi, F. Feki, S. Sayadi, Detoxification of olive mill wastewater by electrocoagulation and sedimentation processes, J. Hazard. Mat. 142 (2007) 58–67.
[9] M. Gotsia, N. Kalogerakisa, E. Psillakisa, P. Samarasb, D. Mantzavinos, Electrochemical oxidation of olive oil mill wastewaters, Water Res. 39 (2005) 4177–4187.
[10] F.A. El-Gohary, M.I. Badawy, M.A. El-Khateeb, A.S. El-Kalliny, Integrated treatment of olive mill wastewater (OMW) by the combination of Fenton's reaction and anaerobic treatment, J. Hazard. Mater. 162 (2008) 1536–1541.
[11] C. Paredes, J. Cegarra, A. Roig, M.A. Sánchez-Monedero, M.P. Bernal, Characterization of olive mill wastewater (alpechin) and its sludge for agricultural purposes, Biores. Technol. 67 (1999) 111–115.
[12] Ministerio de Medio Ambiente, Anuario de Estadística Agroalimentaria y Pesquera, 2007 http://www.mapa.es/estadistica/pags/anuario/2007/pdf/PDF17_10.pdf.
[13] R. Borja, F. Raposo, B. Rincón, Treatment technologies of liquid and solid wastes from two-phase olive oil mills, Grasas y Aceites 57 (2006) 32–46.
[14] H. Mekki, M. Anderson, E. Amar, G.R. Skerratt, M. BenZina, Olive oil mill waste water as a replacement for fresh water in the manufacture of fired clay bricks, J. Chem. Technol. Biotechnol. 81 (2006) 1419–1425.
[15] H. Mekki, M. Anderson, M. BenZina, E. Ammar, Valorization of olive mill wastewater by its incorporation in building bricks, J. Hazard. Mat. 158 (2008) 308–315.
[16] I. González, E. Galán, A. Miras, P. Aparicio, New uses for brick-making clay materials from the Bailén area (southern Spain), Clay Minerals 33 (1998) 453–465.
[17] J. Jiménez Millán, J.M. Molina, P.A. Ruiz-Ortiz, Mineralogical and sedimentological characterization of clay raw materials and firing transformations in the brick-making industry from the Bailén area (southern Spain), in: M. Ortega, A. López Galindo, I. Palomo (Eds.), Advances in Clay Minerals, Universidad de Granada, Granada, 1998, pp. 230–232.
[18] S.N. Monteiro, C.M.F. Vieira, Effect of oily waste addition to clay ceramic, Ceramics Int. 31 (2005) 353–358.
[19] D.F. Lin, C.H. Weng, Use of sewage sludge ash as brick material, J. Environ. Eng. 127 (2001) 922–927.
[20] C.M.F. Vieira, T.M. Soares, R. Sánchez, S.N. Monteiro, Incorporation of granite waste in red ceramics, Mat. Sci. Eng. A 373 (2004) 115–121.
[21] C. Sheng, J.L.T. Azevedo, Estimating the higher heating value of biomass fuels from basic analysis data, Biomass Bioenergy 28 (2005) 499–507.
[22] M. Fernández, Manual sobre fabricación de baldosas, tejas y ladrillos, Beralamar, S.A., Terrassa, 2000, p. 145.
[23] E. Dinelli, T. Tateo, Sheet silicates as effective carries of heavy metals in the ophiolitic mine area of Vigonzano (northern Italy), Mineralogical Magazine 65 (2001) 121–132.
[24] M. Dondi, B. Fabbri, R. Laviano, Characteristics of the clays utilized in the bricks industry in Apulia and Basilicata (southren Italy), Miner. Petrogr. Acta 35A (1992) 179–189.
[25] B. Fabbri, M. Dondi, La produzione del laterizio in Italia, Faenza Editrice, Roma, 1995, p. 160.
[26] B. Fabbri, C. Fiori, Clays and complementary raw materials for stoneware tiles, Mineral. Petrol. Acta 29 (1985) 535–545.
[27] G. Tar, J.M.F. Ferreira, A.T. Fonseca, Influence of particle size and particle size distribution on drying-shrinkage behaviour of alumina slip cast bodies, Ceramics Int. 25 (1999) 577–580.
[28] V. Beltrán, E. Ferrando, J. García, E. Sánchez, Extruded rustic floor tiles. I. Impact of the composition on the body's behaviour in the prefiring process stages, Tile & Brick Int. 11 (1995) 169–176.
[29] E. Krause, Principes fondamentaux du séchage, in: Le séchage en céramique. Principes et techniques, Septima, Paris, 1977, pp. 132–137.
[30] A.I. Avgustinik, Secado y secaderos, in: Cerámica, Reverté, Madrid, 1983, pp. 222–236.
[31] C. Bohlmann, Additives for the optimization of the processing and product properties. Part 2: Auxiliaries for heavy clay bodies, Ziegel Industrie Int. 7 (1999) 61–66.
[32] E. Rimpel, F. Rehme, Additives to reduce the extrusion moisture and the power consumption in the shaping process, Ziegel Int. Annu. (2004) 41–52.
[33] O. Rentz, A. Schmittinger, R. Jochum, F. Schultmann, Exemplary investigation into the state of practical realisation of integrated environmental protection within the ceramics industry under observance of the IPPC-directive and the development of BAT reference documents, Research project 298 94 313/07, Environmental Research Plan of the Federal Minister for the Environment, Nature Conservation and Safety, French-German Institute for Environmental Research University of Karlsruhe (2001) 44–52.
[34] R. Kretz, Symbols for rock-forming minerals, Am. Mineralogist 68 (1983) 277–279.